Vol 18 No 11, November 2009
1674-1056/2009/18(11)/4960-06

Chinese Physics B

© 2009 Chin. Phys. Soc.
and IOP Publishing Ltd

Fabrication and magnetic properties of $Ni_{0.5}Zn_{0.5}Fe_2O_4$ nanofibres by electrospinning*

Xiang Jun(向 军)†, Shen Xiang-Qian(沈湘黔),
Song Fu-Zhan(宋福展), and Liu Ming-Quan(刘明权)

School of Materials Science and Engineering, Jiangsu University, Zhenjiang 212013, *China*

(Received 30 November 2008; revised manuscript received 5 March 2009)

NiZn ferrite/polyvinylpyrrolidone composite fibres were prepared by sol–gel assisted electrospinning. $Ni_{0.5}Zn_{0.5}Fe_2O_4$ nanofibres with a pure cubic spinel structure were obtained subsequently by calcination of the composite fibres at high temperatures. This paper investigates the thermal decomposition process, structures and morphologies of the electrospun composite fibres and the calcined $Ni_{0.5}Zn_{0.5}Fe_2O_4$ nanofibres at different temperatures by thermogravimetric and differential thermal analysis, x-ray diffraction, Fourier transform infrared spectroscopy and field emission scanning electron microscopy. The magnetic behaviour of the resultant nanofibres was studied by a vibrating sample magnetometer. It is found that the grain sizes of the nanofibres increase significantly and the nanofibre morphology gradually transforms from a porous structure to a necklace-like nanostructure with the increase of calcination temperature. The $Ni_{0.5}Zn_{0.5}Fe_2O_4$ nanofibres obtained at 1000 °C for 2 h are characterized by a necklace-like morphology and diameters of 100–200 nm. The saturation magnetization of the random $Ni_{0.5}Zn_{0.5}Fe_2O_4$ nanofibres increases from 46.5 to 90.2 emu/g when the calcination temperature increases from 450 to 1000 °C. The coercivity reaches a maximum value of 11.0 kA/m at a calcination temperature of 600 °C. Due to the shape anisotropy, the aligned $Ni_{0.5}Zn_{0.5}Fe_2O_4$ nanofibres exhibit an obvious magnetic anisotropy and the ease magnetizing direction is parallel to the nanofibre axis.

Keywords: NiZn ferrite nanofibre, electrospinning, magnetic property, shape anisotropy

PACC: 6146, 7500, 8116, 7530G

1. Introduction

NiZn ferrite is one of the most versatile soft magnetic materials among the various spinel ferrites due to its high resistivity and permeability, low dielectric loss, high Curie temperature, etc.[1] Up to now, many research groups have been involved in enhancing the magnetic and electromagnetic properties of NiZn ferrite. Thin films, nanoparticles, nanowires and nanotubes of NiZn ferrites have been prepared by sputtering,[2] spin-spraying,[3] spray pyrolysis,[4] pulsed laser deposition,[5] sol–gel,[6] the combustion method,[7] co-precipitation,[8] the template method[9] and other methods, but NiZn ferrite nanofibres have not been reported in the literature. Therefore, the fabrication of NiZn ferrite nanofibres and research into their magnetic and electromagnetic properties will be of great interest.

Recently, the nanofibrization of materials has attracted much attention due to their large specific surface area, high aspect ratio and obvious anisotropy. Electrospinning has been proved to be a versatile and effective technology for manufacturing microscale to nanoscale fibres. A variety of material nanofibres, such as polymers,[10] metal oxides[11] and hybrid (organic/inorganic) compounds[12] have been prepared via electrospinning. Some spinel simple ferrites with the general formula AFe_2O_4 (A = Co, Ni, Zn, Mn, Cu) were prepared by the eletrospinning process.[13−17] In this study, we have investigated the feasibility of fabrication of spinel NiZn ferrite nanofibres using the electrospinning process of sol–gel solution. The structure, morphology and magnetic properties of the resultant nanofibres are characterized and discussed.

2. Experimental

The fabrication of $Ni_{0.5}Zn_{0.5}Fe_2O_4$ nanofibres consisted of solution preparation, electrospinning and calcination. In the solution preparation, 0.5 g of polyvinylpyrrolidone (PVP, M_w = 1300000, Aldrich) was dissolved in 4.5 g of ethanol. Then 0.311 g nickel acetate ($Ni(CH_3COO)_2{\cdot}4H_2O$), 0.2744 g zinc acetate ($Zn(CH_3COO)_2{\cdot}2H_2O$), 2.02 g ferric nitrate ($Fe(NO_3)_3{\cdot}9H_2O$), and 2 ml deionized water were

*Project supported by the National Natural Science Foundation of China (Grant No 50674048) and the Aerospace Science Foundation of China (Grant No 2007ZF52062).

†Corresponding author. E-mail: junx93@sina.com

added into the PVP/ethanol solution and magnetically stirred for about 24 h at room temperature to form a homogeneous viscous solution ([PVP] = 5.2 wt%, Ni:Zn:Fe = 1:1:4) for electrospinning. The apparatus used for this electrospinning was similar to that in Ref.[18]. The viscous solution was loaded into a plastic syringe with a stainless steel needle. The needle as the positive electrode was connected to a high-voltage supply and the solution was fed at a rate of 0.5 mL/h by using a syringe pump during the electrospinning process. A piece of aluminium foil as the ground collector was placed below the tip of the needle to collect the composite fibres. The distance between the positive electrode and the ground collector was 12 cm and the applied voltage was 12.5 kV. The collected as-spun $Ni_{0.5}Zn_{0.5}Fe_2O_4$/PVP composite fibres were dried and calcined at 450–1000 °C for 2 h in ambient atmosphere.

Thermo-gravimetric and differential thermal analysis (TG/DTA) was carried out on a Perkin Elemer Pyris Diamond TG/DTA thermal analyser at a heating rate of 10 °C/min under air atmosphere. The x-ray diffraction (XRD) patterns were collected on a Bruker D8 advance powder diffractometer with CuKα radiation. Fourier transform infrared spectroscopy (FTIR) spectra of the samples (as pellets in KBr) were recorded by a Nexu670 spectrometer in a wavenumber range of 400–4000 cm^{-1} at a resolution of 4 cm^{-1}. Field emission scanning electron microscopy (FESEM, JSM-7001F) was used to characterize the morphology of the as-spun and calcined fibres. The magnetic properties of the random and aligned $Ni_{0.5}Zn_{0.5}Fe_2O_4$ nanofibres were investigated at room temperature by using a vibrating sample magnetometer (VSM).

3. Results and discussion

3.1. Thermal decomposition process

The thermal behaviour of $Ni_{0.5}Zn_{0.5}Fe_2O_4$/PVP composite fibres is shown in Fig.1. It can be seen that the thermal decomposition process of the $Ni_{0.5}Zn_{0.5}Fe_2O_4$/PVP composite fibres can be divided into three stages. The first stage takes place in the range of 50–140 °C, with a weight loss of about 7% corresponding to a broad endothermic event due to the evaporation of absorbed water and trapped solvent from the composite fibres. A weight loss of approximately 31% occurs during the second stage in the range of 140–230 °C, corresponding to an endothermic event at about 180 °C, which is assigned to a partial decomposition of ferric nitrate, nickel acetate and zinc acetate. The following weight loss of about 35% in the third stage taking place in the range of 230–430 °C corresponds to a very strong endothermic event in the vicinity of 320 °C owing to the further decomposition of remained nitrate and acetate and degradation of PVP, after which there is almost no change in weight loss, indicating the formation of crystalline $Ni_{0.5}Zn_{0.5}Fe_2O_4$ as the decomposition product.

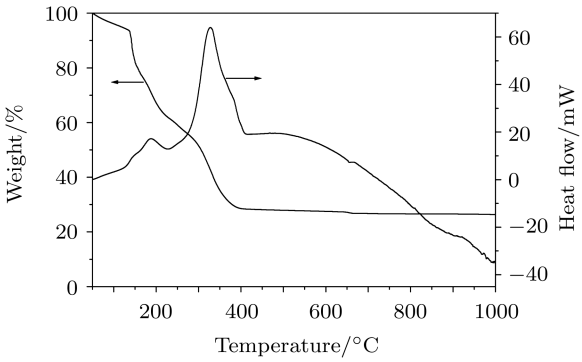


Fig.1. TG/DTA curves of $Ni_{0.5}Zn_{0.5}Fe_2O_4$/PVP composite fibres.

3.2. FTIR spectra

Figure 2 shows FTIR spectra of the $Ni_{0.5}Zn_{0.5}Fe_2O_4$/PVP composite fibres and the calcined products at different calcination temperatures. The spectrum of the as-spun composite fibres (curve *a* of Fig.2) shows some strong absorption characteristic peaks in the region of 600–3000 cm^{-1}, corresponding to the stretching and bending vibrations of PVP, and the band at about 3440 cm^{-1} is ascribed to the O–H stretching vibration of H_2O.[19] After calcination at 450 °C, as shown in curve *b* of Fig.2, most of the peaks assigned to organic materials disappear owing to the decomposition of PVP and a new characteristic peak occurs in the region of 500–700 cm^{-1} due to the stretching mode of Fe–O at tetrahedral sites in the spinel structure, which indicates that the spinel structure begins to form.[13,17,20] As the temperature increases up to 800 °C (curve *d* of Fig.2), only the characteristic peak of the spinel-type ferrite at around 576 cm^{-1} is detected, implying the formation of well-crystallized $Ni_{0.5}Zn_{0.5}Fe_2O_4$ spinel phase and this can be further proved by the XRD results (Fig.3).

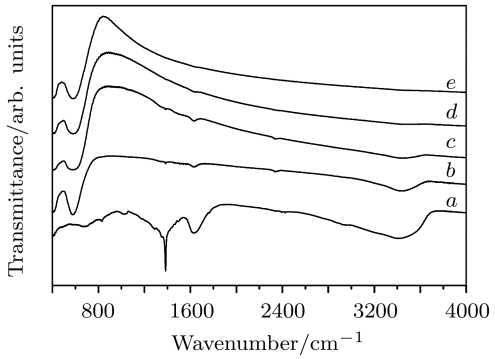


Fig.2. The FTIR spectra of $Ni_{0.5}Zn_{0.5}Fe_2O_4$/PVP composite fibres and the products at different calcination temperatures: Curve *a* as-spun composite fibres; curve *b* 450 °C; curve *c* 600 °C; curve *d* 800 °C; and curve *e* 1000 °C.

3.3. Phase identification

Figure 3 is the XRD patterns of the as-spun composite fibres and the $Ni_{0.5}Zn_{0.5}Fe_2O_4$ nanofibres calcined in air for 2 h under different temperatures. As shown in curve *a* of Fig.3, the as-prepared composite fibres show a typical amorphous structure. After calcination at 450 °C for 2 h (curve *b* of Fig.3), all of the peaks can be indexed to the cubic spinel phase of $(Ni,Zn)Fe_2O_4$ (JCPDS No.08-0234), whilst the crystallinity is still relatively low. With the increase of calcination temperature, the corresponding peaks become sharper and narrow, which implies that the crystallinity is higher and the grain size is larger at high calcination temperatures. In addition, XRD results also show that the as-prepared $Ni_{0.5}Zn_{0.5}Fe_2O_4$ nanofibres are polycrystalline structures almost without a preferred crystallite orientation.

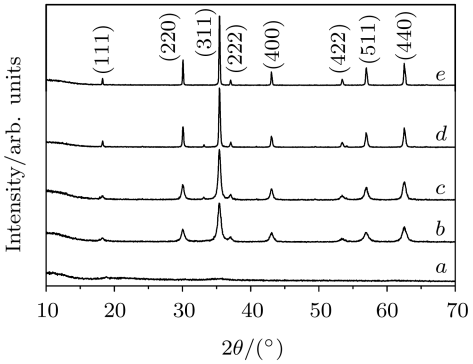
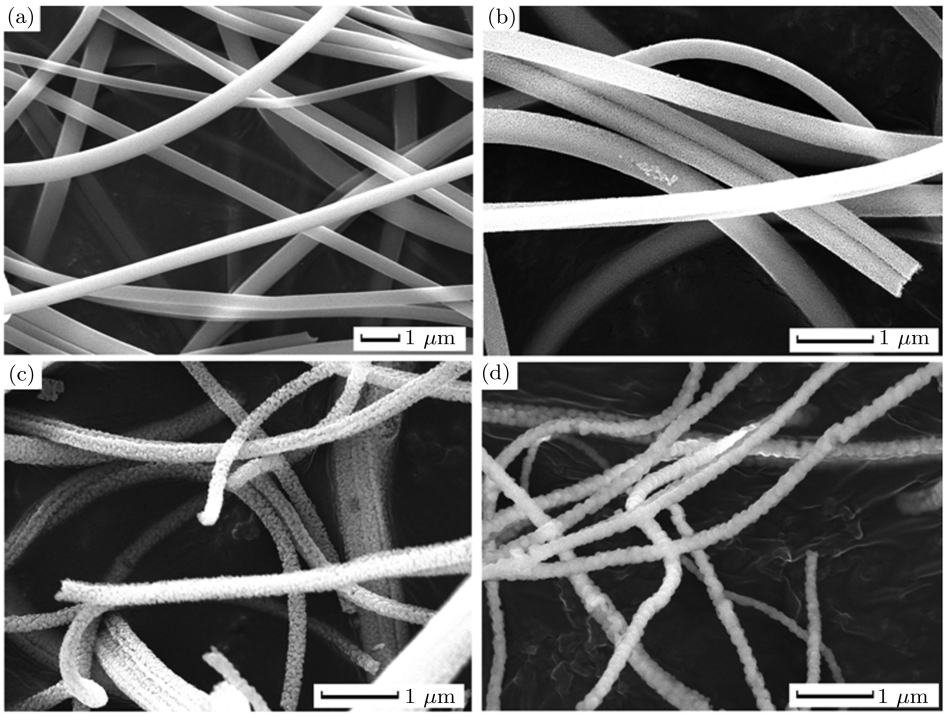


Fig.3. The XRD patterns of $Ni_{0.5}Zn_{0.5}Fe_2O_4$/PVP composite fibres and the products at different calcination temperatures: Curve *a* as-spun composite fibres; curve *b* 450 °C; curve *c* 600 °C; curve *d* 800 °C; and curve *e* 1000 °C.

3.4. Morphology observation

The SEM morphologies of the $Ni_{0.5}Zn_{0.5}Fe_2O_4$ /PVP composite fibres and the fibres obtained at different calcination temperatures are shown in Fig.4.



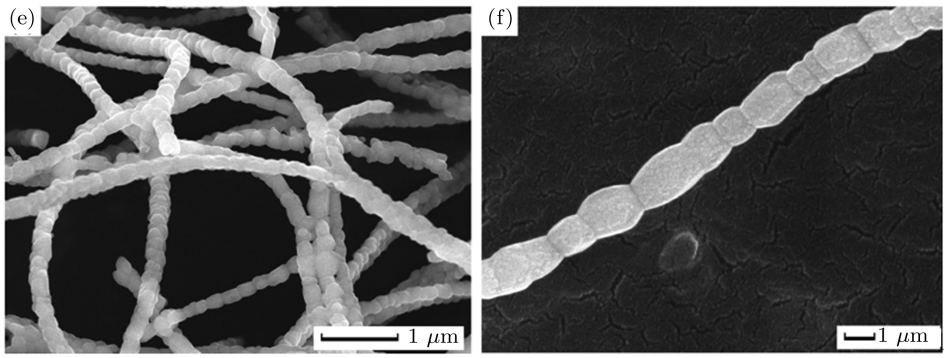


Fig.4. The SEM morphologies of $Ni_{0.5}Zn_{0.5}Fe_2O_4$/PVP composite fibres and the products at different calcination temperatures: (a) as-spun composite fibres; (b) 450 °C; (c) 600 °C; (d) 800 °C; (e) 1000 °C; (f) high-magnification micrograph of a single $Ni_{0.5}Zn_{0.5}Fe_2O_4$ nanofibre calcined at 1000 °C for 2 h.

The surface of dried $Ni_{0.5}Zn_{0.5}Fe_2O_4$/PVP composite fibres is smooth due to the amorphous nature of the composite fibres and their diameters basically range from 400 to 700 nm (Fig.4(a)). The fibre diameters gradually decrease with increasing calcination temperature. After calcination at 450 °C (Fig.4(b)) and 600 °C (Fig.4(c)) for 2 h, the fibre surface shrinks and becomes porous largely owing to the decomposition of PVP and crystallization of spinel $Ni_{0.5}Zn_{0.5}Fe_2O_4$. After calcination at 800 °C for 2 h (Fig.4(d)), the pores on fibre surfaces basically disappear and the fibre diameters decrease to around 250 nm. The cross section of the fibres obtained at this temperature is composed of only several grains with an average size of about 80 nm. The fibre morphology gradually transforms from a porous structure to a necklace-like nanostructure due to growth of the $Ni_{0.5}Zn_{0.5}Fe_2O_4$ grains. When calcination temperature increases to 1000 °C, it can be seen from Figs.4(e) and 4(f) that the $Ni_{0.5}Zn_{0.5}Fe_2O_4$ fibres are mainly necklace-like well-crystallized nanofibres. These necklace-like nanofibres are characterized by diameters in the range of 100–200 nm and an aspect ratio (length/diameter) ranging approximately from 10^3 to 10^4. The formation of necklace-like morphology may be attributed to the asymmetric shrinkage of $Ni_{0.5}Zn_{0.5}Fe_2O_4$ during the thermal decomposition and crystallization process of composite fibres. With the rapid growth of grains during the calcinations at high temperatures, the nanofibres are no longer stable and grain boundary decohesion occurs to relieve the strain energy,[21] leading to the formation of necklace-like nanofibres.

3.5. Magnetic properties

A hysteresis measurement was made to determine saturation magnetization (M_s) and coercivity (H_c). Figure 5 shows the hysteresis loops of the randomly oriented $Ni_{0.5}Zn_{0.5}Fe_2O_4$ nanofibres obtained at different calcination temperatures. All the specimens exhibit a typical soft magnetic characteristic, the magnetization nearly reaches saturation at an external field

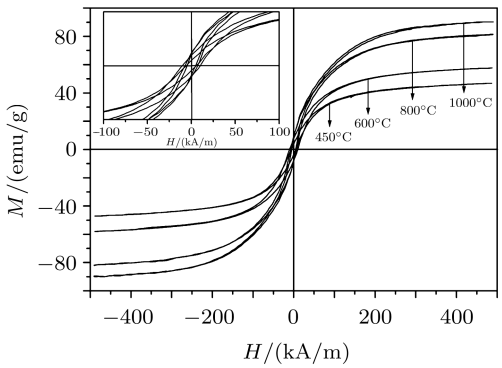


Fig.5. Hysteresis loops of the randomly oriented $Ni_{0.5}Zn_{0.5}Fe_2O_4$ nanofibres obtained at different calcination temperatures. Inset shows enlarged partial hysteresis curves and coercivity in detail.

of ∼250 kA/m. The variations of saturation magnetization and coercivity of these $Ni_{0.5}Zn_{0.5}Fe_2O_4$ nanofibres with calcination temperature are presented in Table 1. It can be seen that the saturation magnetization increases from 46.5 to 90.2 emu/g as calcination temperature increases from 450 to 1000 °C. This phenomenon may be attributed to the enhancement of the fibre purity and crystallinity and a decreasing proportion of the pinned surface magnetic moments in overall magnetization as the nanocrystals grow in size.[22]

Corresponding to the nanocrystal growth process, coercivity increases initially with the calcination temperature and reaches a maximum value at around 600 °C. Afterward, the coercivity begins to decrease with a further increase of calcination temperature. This indicates that the transformation from single-domain to multi-domain will occur in the magnetic domain structure of $Ni_{0.5}Zn_{0.5}Fe_2O_4$ nanofibres with the increase of calcination temperature.

Table 1. Magnetic properties of the randomly oriented nanofibres calcined at different temperatures for 2 h.

calcination temperature/°C	M_s/(emu/g)	H_c/(kA/m)
450	46.5	5.7
600	57.6	11.0
800	81.4	7.4
1000	90.2	4.4

For the randomly oriented $Ni_{0.5}Zn_{0.5}Fe_2O_4$ nanofibres, the coercivity should be primarily due to the contribution from magnetocrystalline anisotropy but the shape anisotropy. It was reported that the crystal particle can be considered as a single domain when the crystal particle size is smaller than 62 nm.[23] In this work, when the calcination temperature is relatively low, the grain size is very small and below the critical single-domain size. According to Stoner–Wohlfarth single domain theory,[24] the magnetocrystalline anisotropy energy (E_A) of a nanocrystal single domain is approximated by

$$E_A = KV \sin^2 \theta, \tag{1}$$

where K is an anisotropy constant, V is the volume of the nanocrystal, and θ is the angle between the ease axis and the direction of field-induced magnetization. The increase in coercivity of the $Ni_{0.5}Zn_{0.5}Fe_2O_4$ nanofibres initially with increasing calcination temperature can be explained by the increase in magnetocrystalline anisotropy. When the calcination temperature is above 600 °C, the $Ni_{0.5}Zn_{0.5}Fe_2O_4$ nanocrystals contained in fibres are larger than the single-domain size and reach multi-domains due to the rapid increase in grain size, and the formation of domain walls will cause the coercivity to decrease.[25] This decrease of coercivity is usually attributed to a switch of the magnetization process from domain rotation to domain wall motion. At the same time, with further increase in the calcination temperature from 600 to 1000 °C, the concentration of impurities and defects in these nanofibres will gradually decrease owing to an improvement in the nanofibre's crystallization, which is beneficial to reduce the resistance of domain wall motion and consequently leads to a monotonous decrease in coercivity.

For magnetic nanowire arrays or aligned nanofibres, the shape anisotropy may compete with the magnetocrystalline anisotropy and play an important role in the magnetic properties.[26] In order to study preliminarily the effect of shape anisotropy on nanofibre magnetization behaviour, the as-obtained $Ni_{0.5}Zn_{0.5}Fe_2O_4$ nanofibres were dispersed into a melted paraffin solution under a constant magnetic field and then solidified to form a largely aligned nanofibre sample. The hysteresis loops of the aligned $Ni_{0.5}Zn_{0.5}Fe_2O_4$ nanofibres calcined at 1000 °C for 2 h are shown in Fig.6, where // and ⊥ show that the applied field H is parallel and perpendicular to the nanofibre axis, respectively. The different shapes of the hysteresis loops in the parallel and perpendicular directions indicate that the aligned nanofibres exhibit an obvious anisotropy. The magnetic field required to reach the saturated magnetization is higher in the perpendicular case. The squareness ratio and coercivity for these aligned nanofibres in parallel are 0.34 and 2.8 kA/m, and in perpendicular 0.12 and 4.5 kA/m, respectively. From these data, the magnetization for the aligned nanofibres in parallel is softer with a relatively higher squareness ratio in comparison with that of the aligned nanofibres in perpendicular. This implies that the shape anisotropy is slightly dominant in the competition with the magnetocrystalline anisotropy in determining the ease axis of magnetization for the aligned $Ni_{0.5}Zn_{0.5}Fe_2O_4$ nanofibres.

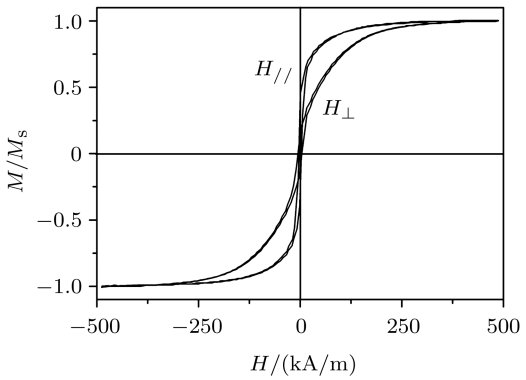


Fig.6. Hysteresis loops of the aligned $Ni_{0.5}Zn_{0.5}Fe_2O_4$ nanofibre sample with the applied field parallel ($H_{//}$) and perpendicular ($H_\perp$) to the nanofibre axis.

4. Conclusions

$Ni_{0.5}Zn_{0.5}Fe_2O_4$ nanofibres with a pure cubic spinel structure were successfully fabricated by use of the sol–gel assisted electrospinning process. The morphology and diameters of the fibres are largely affected by the calcination temperature. With increasing calcination temperature, the morphology of the calcined fibres gradually transforms from a porous structure to a necklace-like nanostructure. The $Ni_{0.5}Zn_{0.5}Fe_2O_4$ fibres calcined at 1000 °C for 2 h are mainly necklace-like nanofibres with diameters of 100–200 nm and aspect ratios ranging from 10^3 to 10^4. The magnetic measurement shows that the saturation magnetization of the randomly oriented nanofibres increases with increasing temperature, while the corcivity reaches a maximum value at a calcination temperature of about 600 °C. The aligned $Ni_{0.5}Zn_{0.5}Fe_2O_4$ nanofibres exhibit an obvious shape anisotropy. This shape anisotropy, competing with the magnetocrystalline anisotropy, is slightly dominant in determining the ease axis of magnetization along the nanofibre axis.

References

[1] Deka S and Joy P A 2006 *Mater. Chem. Phys.* **100** 98

[2] Gao J H, Cui Y T and Yang Z 2004 *Mater. Sci. Eng.* B **110** 111

[3] Kondo K, Chiba T, Ono H, Yoshida S, Shimada Y, Matsushita N and Abe M 2006 *J. Magn. Magn. Mater.* **301** 107

[4] Takayama A, Okuya M and Kaneko S 2004 *Solid State Ionics* **172** 257

[5] Welch R G, Neamtu J, Rogalski M S and Palmer S B 1996 *Solid State Commum.* **97** 355

[6] He X H, Song G S and Zhu J H 2005 *Mater. Lett.* **59** 1941

[7] Azadmanjiri J 2008 *Mater. Chem. Phys.* **109** 109

[8] Gul I H, Ahmed W and Maqsood A 2008 *J. Magn. Magn. Mater.* **320** 270

[9] Yu M, Liu J H and Li S M 2007 *J. Univ. Sci. Tchnol. Beijing* **14** 469

[10] Bognitzki M, Czado W, Frese T, Schaper A, Hellwig M, Steinhart M, Greiner A and Wendorff J H 2001 *Adv. Mater.* **13** 70

[11] Li J Y, Tan Y, Xu F M, Sun Y, Cao X Q and Zhang Y F 2008 *Mater. Lett.* **62** 2396

[12] Lu X F, Li L L, Zhang W J and Wang C 2005 *Nanotechnology* **16** 2233

[13] Ju Y W, Park J H, Jung H R, Cho S J and Lee W J 2008 *Mater. Sci. Eng.* B **147** 7

[14] Li D, Herricks T and Xia Y N 2003 *Appl. Phys. Lett.* **83** 4586

[15] Zhan S H, Gong C R, Chen D R and Jiao X L 2006 *J. Disper. Sci. Technol.* **27** 931

[16] Ju Y W, Park J H, Jung H R, Cho S J and Lee W J 2008 *Compos. Sci. Technol.* **68** 1704

[17] Ponhan W and Maensiri S 2008 *Solid State Sci.* **11** 479

[18] Yuh J, Perez L, Sigmund W M and Nino J C 2007 *Phys.* E **37** 254

[19] Sun Y, Li J Y, Tan Y and Zhang L 2008 *J. Alloys. Comp.* **471** 400

[20] Wu K H, Shin Y M, Yang C C, Wang G P and Horng D N 2006 *Mater. Lett.* **60** 2707

[21] Lu X F, Zhang D L, Zhao Q D, Wang C, Zhang W J and Wei Y 2006 *Macromol. Rapid Commum.* **27** 76

[22] Song Q and Zhang Z J 2004 *J. Am. Chem. Soc.* **126** 6164

[23] Liu Y and Qin T 2007 *Chin. Phys.* **16** 3837

[24] Stoner E C and Wohlfarth E P 1991 *IEEE Trans. Magn.* **27** 3475

[25] Maaz K, Mumtaz A, Hasanain S K and Ceylan A 2007 *J. Magn. Magn. Mater.* **308** 289

[26] Hu H N, Yang C H, Chen J L and Wu G H 2008 *J. Magn. Magn. Mater.* **320** 2305